Use of electrophoretic mobility to determine the secondary structure of a small antisense RNA

Jean-Philippe Jacques+ and Miriam M.Susskind*
Department of Biological Sciences, University of Southern California, Los Angeles, CA 90089-1340, USA

Received February 21, 1991; Revised and Accepted April 11, 1991

ABSTRACT

Natural antisense RNAs have stem-loop (hairpin) secondary structures that are important for their function. The *sar* antisense RNA of phage P22 is unusual: the 3′ half of the molecule forms an extensive stem-loop, but potential structures for the 5′ half are not predicted to be thermodynamically stable. We devised a novel method to determine the secondary structure of *sar* RNA by examining the electrophoretic mobility on non-denaturing gels of numerous *sar* mutants. The results show that the wild-type RNA forms a 5′ stem-loop that enhances electrophoretic mobility. All mutations that disrupt the stem of this hairpin decrease mobility of the RNA. In contrast, mutations that change the sequence of the stem without disrupting it (e.g. change G·U to A·U) do not affect mobility. Nearly all mutations in single-stranded regions of the structure also have no effect on mobility. Confirmation of the proposed 5′ stem-loop was obtained by constructing and analyzing compensatory double mutants. Combinations of mutations that restore a base-pair of the stem also restore mobility. The genetic phenotypes of *sar* mutants confirm that the proposed secondary structure is correct and is essential for optimal activity of the antisense RNA in vivo.

INTRODUCTION

The *sar* gene of phage P22 encodes a small antisense regulatory RNA that represses expression of the adjacent antirepressor (*ant*) gene at a post-transcriptional level (1, 2). Whereas *ant* mRNA is transcribed rightward from the *ant* promoter (P_{ant}), *sar* RNA is transcribed in the opposite direction from P_{sar}, a promoter within the *ant* coding sequence. Transcription from P_{sar} terminates micro-heterogeneously at a strong, Rho-independent transcription terminator, T_{sar}. Full-length *sar* RNA is 68–69 nt long (Fig. 1), and is complementary over its entire length to the intercistronic region of the mRNA between the end of *arc* (the first gene in the *ant* operon) and the start of *ant*, including the *ant* ribosome binding site (Fig. 2).

Studies of other naturally-occurring antisense RNAs emphasize that these small molecules have extensive secondary structures that are important for their mechanism of action (3). Usually, most of the RNA molecule is folded into one to three stem-loop (hairpin) structures. The hairpin loops are used for rapid, initial pairing ('kissing') between the antisense and target RNAs. Another role of the extensive secondary structure is to protect the free antisense RNA from nucleolytic degradation in vivo (4).

In the case of *sar* RNA, the 3′ half of the molecule consists of the T_{sar} terminator stem-loop (1; Fig 1). This extensive 3′ structure is predicted to be thermodynamically stable because it consists of a small loop and a long stem containing four contiguous strong base-pairs (5, 6). However, the sequence of the 5′ half of *sar* does not suggest any striking or even stable structure. Fig. 1 illustrates the alternative potential structures I and II; their derivatives I′ and II′ (see Fig. 8) have extended 5′ stems interrupted by interior loops (mismatched bases in both strands). All of these potential 5′ structures are characterized by short, weak-looking duplexes and numerous unpaired bases in the loops. Hence, the calculated free energies of these 5′ structures are close to 0 ($\Delta G(25°C) = -0.6$ to $+3.7$ kcal/mol). Thus, none of these structures is predicted to be thermodynamically stable in solution, based on current methods for predicting RNA secondary structure.

Preliminary experiments probing the secondary structure of *sar* RNA by RNase attack in vitro (7) and analysis of a few 5′-proximal *sar* mutations in vivo (8) were previously reported informally. These studies confirmed the presence of the T_{sar} stem-loop, but only tentatively pointed to the formation of the 5′ stem-loop of structure II (Fig. 1). It was noted that some of the nuclease attack experiments were inconsistent with this secondary structure: (i) RNase V1, a double-strand specific enzyme, cleaved within the 5′ loop (position 24); and (ii) RNase A, a single-strand specific enzyme, did not cleave in a pyrimidine-rich stretch of the 5′ loop (positions 20–25) (7).

While analyzing a large collection of new *sar* mutations, we serendipitously found that many of these mutations substantially affect the mobility of *sar* RNA on non-denaturing gels. These preliminary findings prompted us to systematically investigate the feasibility of using electrophoretic mobility as a method to

* To whom correspondence should be addressed

+ Present address: Department of Microbiology, University of Geneva Medical School, 9 Ave de Champel, CH1211 Geneva, Switzerland

determine the secondary structure of *sar* RNA. We describe the analysis of numerous *sar* alleles, including single mutations specifically designed to test alternative models, and combinations of mutations predicted to be (or not to be) compensatory. Without exception, these results lead to the conclusion that the wild-type RNA forms structure I in solution, and that this structure enhances mobility of the molecule in non-denaturing gels. These findings are reminiscent of the well-established idea that local stem-loops in single-stranded RNA or DNA can cause band compressions in sequencing gels (9–12). Finally, analysis of *sar* mutants in vivo fully supports the hypothesis that structure I forms in vivo, and is essential for optimal *sar* RNA activity.

MATERIALS AND METHODS

Plasmids and nomenclature

Plasmids carrying the *sar* gene are derivatives of the closely related plasmids pMS390, pMS610 and pMS659 (13). Several of the *sar* mutations used here were described previously (8, 13). The others were obtained by oligonucleotide-directed mutagenesis of pMS659 using the Amersham Corp. mutagenesis system, version 2. Each mutation is designated by the sequence change it induces in *sar* RNA, preceded by its position. Deletions of one of a run of identical base-pairs are arbitrarily named 4Δ (also called 5Δ) and 8Δ. For double mutants, the two mutations are separated by a slash.

Transcription in vitro

The *sar* region of plasmids was amplified by PCR (14) to generate a 278-bp DNA fragment, which was used as template for transcription in vitro. The fragment extends from −109 to +169 relative to the startpoint of P_{sar}. Transcription reactions were carried out in a total volume of 40 μl, containing 20 mM TrisHCl (pH 8), 100 mM KCl, 10 mM $MgCl_2$, 1 mM dithiothreitol, 100 μg/ml acetylated bovine serum albumin (gift from D.Galas), 0.6 nM DNA and 5 nM RNA polymerase (gift from J.Ding and C.A.Gross). Transcripts were labelled with [α-^{32}P]UTP (Amersham Corp.) under standard conditions in the presence of all 4 NTPs (200 μM each). Reactions were initiated by addition of enzyme and terminated after 30 min at 37°C by addition of 4 μl of freshly made stop solution (50% glycerol, 0.25% bromophenol blue, 250 mM EDTA).

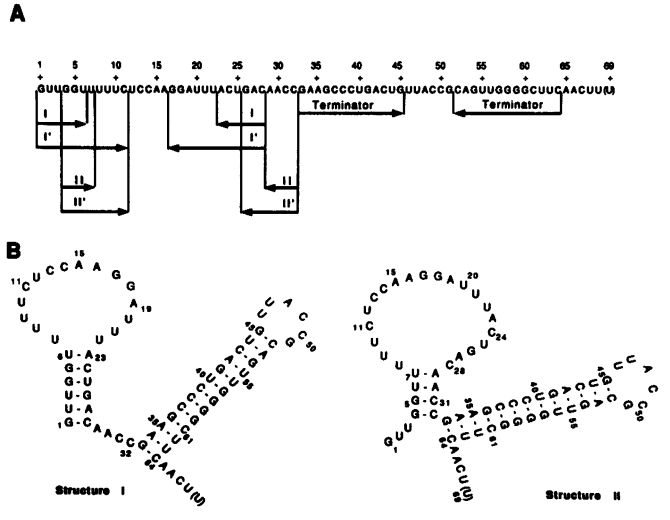

Figure 1. Primary and secondary structure of *sar* RNA. (A) Sequence of *sar* RNA. Termination occurs predominantly at positions 68 and 69, as indicated by the last U in parentheses. Inverted repeats most probably involved in formation of secondary structures are indicated by arrows below the sequence. Structures I′ and II′ are extended versions of structures I and II (see Fig. 8). (B) Secondary structures I and II. Hyphens represent base-pairings; G·U base-pairs are allowed.

Electrophoresis

Transcription products were resolved by electrophoresis in 8% polyacrylamide (25:1 acrylamide:bisacrylamide) wedge gels (0.25–0.75 mm thick) on a Poker-face sequencing apparatus (Hoefer Sci.). Denaturing gels contained 45 mM Tris-borate, 0.5 mM EDTA, 7 M urea, and were prepared according to standard methods using a 20×Tris-borate-EDTA (TBE) stock solution (pH 8.3). The running buffer (1×TBE) was not re-circulated, and electrophoresis was carried out at room temperature. The voltage was adjusted periodically to keep the temperature of the gel itself constant at 40 ± 1°C, measured at the top of the gel by inserting an alcohol thermometer under the safety cover and through the upper buffer reservoir. Non-denaturing gels contained 1×TBE without urea and were run in 1×TBE buffer in a cold room (5°C). The temperature at the top of the gel was kept constant at 20 ± 1°C as described above. The products of transcription reactions were run next to a poly(U) ladder, which served as a convenient 'ruler' for measuring mobility shifts. This ^{32}P-labelled poly(U) ladder was generated by pseudo-templated transcription at the *sar+1T* mutant promoter by *E.coli* RNA polymerase (13). Both denaturing and non-denaturing gels were run until the bromophenol blue tracking dye had migrated 23 cm; the wild-type *sar* transcripts migrated slightly behind (20–21 cm). After drying, gels were autoradiographed using Kodak XAR-5 film.

Characterization in vivo

S.typhimurium strain MS1868 (15) was lysogenized with P22 *Kn6 P_{ant}-32C arc-amH1605 lac2 9-delTB*, generating MS3166. The prophage, which has been described in detail (16), carries a substitution that replaces an internal fragment of the *ant* gene with *E.coli lac 'Z-Y-A'* sequences, generating an *ant/lacZ* gene fusion. This operon is transcribed constitutively from a mutant *ant* promoter (−32A→C); the prophage does not produce the transcriptional repressors of P_{ant} (17) because the *Kn6*

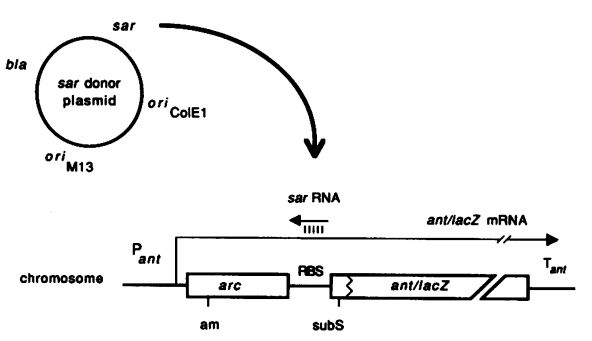

Figure 2. Repression of an *ant/lacZ* gene fusion in vivo by *sar* RNA. Open boxes represent genes of interest in the modified *ant* operon of a P22 *ant/lacZ* prophage. Base-pairing between *sar* RNA (leftward arrow) and *ant* mRNA (rightward arrow) is indicated by vertical lines. The *ant/lacZ* prophage does not produce the transcriptional repressors of P_{ant} because the *mnt* gene is deleted and the *arc* gene is inactivated by an amber mutation (*am*). The *ant/lacZ* fusion does not produce *sar* RNA because a 4-bp substitution (*subS*) inactivates the *sar* promoter.

substitution deletes the *mnt* gene and an amber mutation inactivates the *arc* gene. The *ant/lacZ* fusion does not produce *sar* RNA because the *sar* promoter has been inactivated by a 4-bp substitution (P_{sar}-*subS*) in the −10 region. However, the *ant/lacZ* gene is sensitive to repression by *sar* RNA provided in trans by a *sar* plasmid (Fig. 2).

Derivatives of MS3166 freshly transformed with various monomeric *sar* plasmids (derivatives of pMS659) were used. Overnight cultures were grown in M9CAA (18) containing ampicillin (50 μg/ml), and were diluted 100-fold in the same medium. These cultures were grown at 37°C to mid-log phase (OD_{600} ~0.3), and were harvested and assayed for β-galactosidase activity in microtiter plates as described previously (16). Each strain was assayed 2−4 times, and the parental strain MS3166 was always assayed in parallel (without ampicillin). The repression index (RI) for each *sar* genotype is the β-galactosidase activity in the parental strain (ca. 400 Barrick units) divided by that in the plasmid-bearing strain.

RESULTS

Rationale

Electrophoretic mobility under denaturing and non-denaturing conditions was systematically examined for 41 single or double *sar* mutants obtained by UV or site-directed mutagenesis. Fig. 3 shows the results when the wild-type and mutant RNAs, which were synthesized in vitro by *E.coli* RNA polymerase, were run on denaturing (urea-containing) gels. Previously, RNA sequence analysis showed that the two major bands of wild-type *sar* RNA initiate at 1G and terminate at 68U and 69U (1). In the overexposed autoradiographs shown here, slower-moving minor bands are also seen; their origin has not been fully investigated, but all of them can be labelled with [γ-^{32}P]GTP but not [γ-^{32}P]ATP (data not shown). Since the nearest G residues are at −14 and +4, it is likely that these minor transcripts also initiate at 1G and terminate heterogeneously. (The *sar* Rho-independent terminator is unusual in that termination occurs primarily at the first and second of a run of only 3 T residues.) This pattern of bands is similar for all 41 mutants: the doublet of major bands migrates ahead of the minor bands, and the intensities of the two major bands are usually approximately equal. For all but three mutants, the major doublet co-migrates with that of wild-type *sar* RNA. As expected, the doublet runs slightly faster for two mutants that delete a nucleotide (4Δ and 8Δ) and slightly slower for a mutant that inserts a nucleotide (28AA). Hence, none of these mutations affected the start site or termination sites of the major *sar* transcripts. These mutations also did not affect the efficiency of termination at T_{sar}.

The effects of these mutations on electrophoretic mobility under non-denaturing conditions are shown in Fig. 4 and illustrated in Figs. 5−8. Poly(U) of variable length was used as a ruler to measure mobility shifts of mutant *sar* RNAs. Because of their homogeneity and random-coil configuration, these molecules produced an ideal, evenly-spaced RNA 'ladder' on non-denaturing gels. The mobility of the faster-migrating major band of wild-type *sar* RNA was used as reference ($\mu \equiv 0$) for comparison with the corresponding band of mutant RNAs. The μ value for each mutant was obtained by counting the change in length, to the nearest integer, necessary to cause the same shift in mobility of poly(U), either down (+) or up (−) the gel.

For most mutants, the entire bevy of bands shifted as a unit up or down the gel; the two major bands were still the fastest, as in the urea gel. In some cases, two minor bands ran ahead of the major bands in the non-denaturing gel; these were not considered in calculating μ. For 16G, which gave a triplet of major bands on the non-denaturing gel (but not the urea gel), the fastest band of the triplet was used to calculate μ. For 25G, the band migrating one step ahead of the most intense band was used.

Structures I and II: positions 3, 4, 25 and 32

Structure I has 4G paired with 25U (abbreviated 4G·25U) and 3U paired with 26G (3U·26G), whereas structure II has 4G paired with 32C and has 3U unpaired (Fig. 5). The 4C and 4Δ

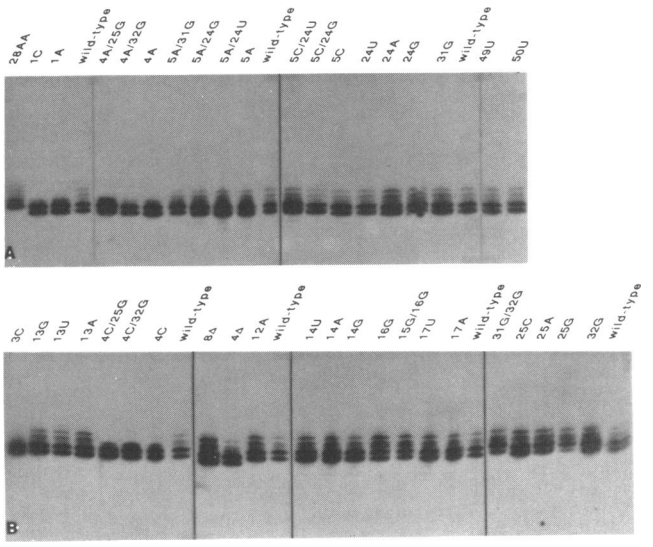

Figure 3. Electrophoretic mobility of *sar* RNA mutants on denaturing gels. Transcription products were resolved on 8% polyacrylamide gels containing urea.

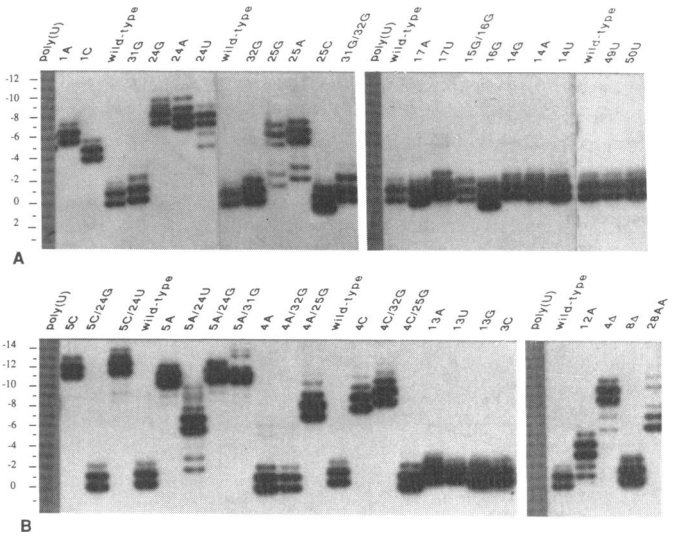

Figure 4. Electrophoretic mobility of *sar* RNA mutants on non-denaturing gels. The same samples used in Fig. 3 were run on 8% polyacrylamide gels without urea. The lanes containing poly(U) were used to measure mobility shifts. These lanes are from longer exposures of the same gels, and were sometimes shifted 1−2 mm with respect to the other lanes to line up the reference *sar* band with the nearest poly(U) band.

mutations, which should disrupt both structures, showed a large decrease in mobility ($\mu = -8$), indicating that these mutations do affect the secondary structure of *sar* RNA. In contrast, mobility was not affected by the 4A mutation, which is predicted to disrupt structure II but improve structure I by changing the non-canonical 4G·25U base-pair to A·U. The 3C mutation is predicted to reinforce structure I by changing the 3U·26G base-pair to C·G, and might affect structure II by allowing 33G to pair with 3C instead of 64C. This mutation also had no effect on mobility. These results established a pattern: (i) μ decreases when a base-pair in the stem of structure I is disrupted; and (ii) μ is not affected when a G·U base-pair in the stem of structure I is changed to A·U or G·C.

This pattern was confirmed when mutations were created that change the bases paired with 4G in either structure I (25U) or structure II (32C). These mutations are particularly informative because they are predicted to affect the stem of either structure I or II, but not both. Position 25 is in the stem of structure I, but is in the loop of structure II; position 32 is in the stem of structure II, but is in the single-stranded 'hinge' between the loops of structure I (Fig. 5). All three changes at position 25 were obtained, and their effects on mobility followed the rules described above. The 25G and 25A mutations, which disrupt the 4G·25U base-pair of structure I, decreased mobility ($\mu = -5$). The 25C mutation, which changes this base-pair from G·U to G·C, had little effect ($\mu = +1$). Finally, the 32G mutation, which would disrupt one of the G·C base-pairs of the stem of structure II, had no effect on μ.

Structures I and II: positions 1, 5, 24 and 31

The effects of additional point mutations in the 5′ half of *sar* RNA are shown in Fig. 6. Without exception, these results support formation of structure I. First, mobility was decreased by mutations that disrupt or weaken the stem of structure I but not II (positions 1 and 24; $\mu = -4$ to -7) and by mutations that disrupt both structures (position 5; $\mu = -8$ to -11). Second, mobility was not affected by mutations predicted to disrupt structure II but not I (31G and 31G/32G; $\mu = 0$). The results obtained with the 31G/32G tandem-double mutant strongly suggest that these positions are not involved in formation of a secondary or tertiary structure.

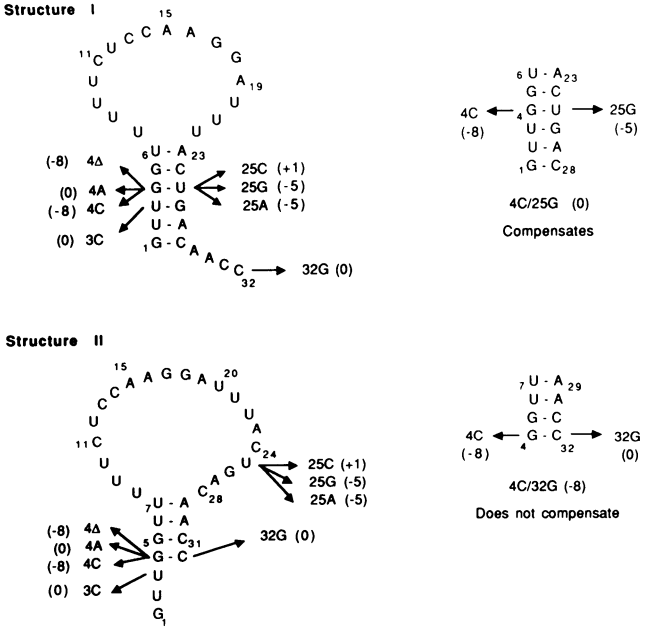

Figure 5. Mutations at positions 3, 4, 25 and 32. The same 8 mutations are shown in the context of structure I (top left) and structure II (bottom left), with μ for each mutation given in parentheses. For clarity, only the 5′ half of *sar* RNA is shown. On the right, pairs of mutations predicted to be compensatory are shown in the context of the stem of either structure I (top right) or II (bottom right). Arrows point to the μ values for each single mutant; the phenotypes of the double mutants are given below each truncated structure.

Compensatory mutations

A powerful method for probing RNA secondary structure is the analysis of double mutations that are predicted to restore a base-pair (compensatory mutations). We constructed the double mutants 4C/25G and 4C/32G, which were predicted to be compensatory according to structure I and II, respectively (Fig. 5). Mobility was fully restored when the 4C and 25G mutations, each of which decreased μ by itself, were combined. In contrast, the 4C/32G combination was non-compensatory: the mobility of the double mutant was the same as that of the slower single mutant. Fig. 6 shows the results obtained when mutations at positions 5 and 24 were combined. The 5C/24G combination fully restored mobility ($\mu = 0$), while the 5A/24U combination partially restored mobility ($\mu = -6$). Hence, these results provide strong evidence for the existence of the fourth and fifth base-pairs of structure I.

Because redundant oligonucleotides were used to construct the double mutants, we also obtained several combinations that were not expected to be compensatory by either model (4A/25G, 4A/32G, 5A/24G, 5C/24U, and 5A/31G). In all of these cases, the mobility of the doubly mutant RNA was either equal to or slightly less than the mobility of the slower single mutant (Fig. 4). In particular, the partially-compensatory behavior of the 5A/24U combination ($\mu = -6$; Fig. 6) is significantly different from the non-compensatory behavior of the 5A/24G, 5C/24U, and 5A/31G combinations ($\mu = -11$).

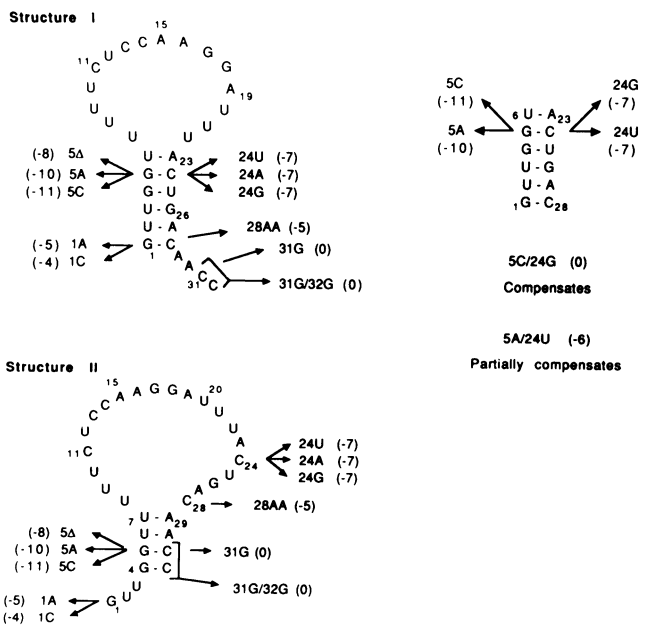

Figure 6. Mutations in *sar* RNA at positions 1, 5, 24, 28 and 31. Eleven mutations are shown in the context of structures I and II as described in the legend to Fig. 5.

Most mutations in the loops have no effect on μ

Ten mutations in the 5′ loop of structure I and two mutations in the loop of the terminator structure had no effect on μ (Fig. 7), suggesting that these positions (13−17, 49 and 50) are not involved in any secondary or tertiary structure detectable by this technique. This argument is strongest for positions 13 and 14 because all three changes at these positions were examined. The only loop mutation that had a significant effect on mobility was 12A (μ = −3).

If interior loops are allowed, some of the bases in the 5′ loop could potentially pair, forming the extended structures I′ or II′ (Figs. 1 and 8). A few of the mutations already described could potentially affect formation of such structures. The 28AA mutation was designed to eliminate the interior loop of structure II′, allowing formation of a structure with an uninterrupted 8-bp stem and 14-nt loop. Similarly, the 12A mutation could potentiate formation of an elongated structure II′ by adding an additional base-pair (12A·25U) at the tip of the stem. If either of these mutant structures is formed, it must retard rather than enhance mobility, since μ = −5 for 28AA and −3 for 12A. An alternative explanation for the 28AA mutation is that it has the same effect as the 1A (μ = −5) and 1C (μ = −4) mutations, which is to disrupt the base-pair at the base of the stem of structure I (Fig. 6).

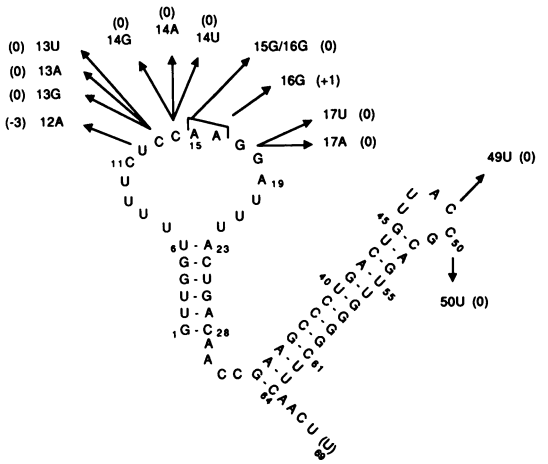

Figure 7. Mutations in the loops of *sar* RNA.

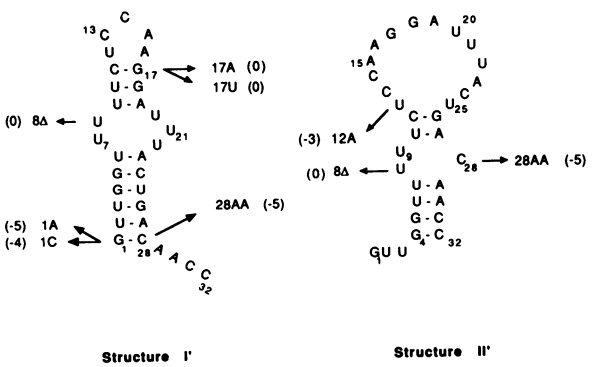

Figure 8. Extended structures I′ and II′. A subset of the mutations are shown in the context of extended secondary structures containing interior loops.

The fact that the 17A and 17U mutations had no effect on mobility argues against structure I′, since these mutations would disrupt the potential 11C·17G base-pair at the tip of the extended stem (Fig. 8). The 8Δ mutation, which would change the conformation of the interior loop of both structures I′ and II′, also had no effect on μ. Hence, these results do not provide any evidence in support of structures I′ and II′. The 17U and 8Δ mutants also argue against an extended structure I in which positions 7−10 are paired with 15−18.

Confirmation of structure I by in vivo analysis

To test the validity of the secondary structure proposed on the basis of mobility, we assayed the effects of some of these mutations on *sar* RNA activity in vivo. In the in vivo system, *sar* RNA provided in trans by a high-copy plasmid represses expression of a single-copy *ant/lacZ* gene fusion carried on a P22 prophage integrated in the Salmonella chromosome (Fig. 2). The steady-state level of β-galactosidase from this fusion was reduced 330-fold (repression index, RI = 330) in the presence of the *sar*$^+$ control plasmid (Table 1). This effect is due to bona fide *sar* RNA initiating at P_{sar} on the plasmid, since no repression occurred (RI = 1) when the plasmid carried P_{sar}−*subS*, a 4-bp substitution that inactivates the *sar* promoter. The results for plasmids carrying various mutations in the *sar* gene show a striking correlation between efficiency of repression in vivo and mobility on non-denaturing gels. All single mutants with normal mobility (μ = 0 or +1) were comparable to the wild type in efficiency of repression (RI ≥ 170), and all single mutants with decreased mobility (μ = −5 to −11) were extremely defective in repression (RI ≥ 12). Moreover, the repression index was high for the fully compensatory double mutants (RI = 210−370), intermediate for the partially

Table 1. Correlation between gel mobility and efficiency of repression

Genotype of *sar* RNA	μ	Repression Index[a]
Wild-type	0	330
P_{sar}-*subS*	NA	1
4A	0	330
4C	−8	8
4C/25G	0	210
4C/32G	−8	7
5A	−10	4
5A/24G	−11	6
5A/24U[b]	−6	45
5C	−11	6
5C/24G	0	370
5C/24U[b]	−11	6
24G	−7	7
24A	−7	8
24U[b]	−7	10
24U	−7	12
25G	−5	6
25A	−5	4
25C	+1	220
31G	0	450
32G	0	170

[a] β-Galactosidase in the absence of *sar* RNA divided by that in the presence of *sar* RNA (see Materials and Methods). [b] These plasmids carry an unprogrammed mutation in the spacer region of P_{sar}, −25C→T, which arose in the site-directed construction of the 24U plasmid and was passed on to its 5A/24U and 5C/24U derivatives. The promoter mutation has no apparent effect, since the 24U/−25T plasmid (line 15) is not significantly different from a 24U plasmid with wild-type P_{sar} (line 16), obtained by repeating the 24U construction.

compensatory double mutant (RI = 45), and low for the non-compensatory double mutants (RI = 6–7). The phenotypes of mutants in the loops will be discussed elsewhere.

DISCUSSION

Secondary structure of *sar* RNA

Structure I is not predicted to be thermodynamically stable, since it has a large (16-nt) hairpin loop and a short (6-bp) stem containing two G·U base-pairs and only two non-adjacent G·C base-pairs. Nevertheless, the results presented here argue strongly that structure I forms in vitro (and presumably in vivo), and makes the RNA run faster in non-denaturing gels. The mobility data can be summarized as follows. (i) Mobility of *sar* RNA is reduced by any of 12 single or tandem-double mutations that disrupt or weaken the first (1G·28C), fourth (4G·25U), or fifth (5G·24C) base-pair of the stem of structure I. (ii) Three single mutations in the stem of structure I have little or no effect on μ. Rather than disrupting a base-pair, each of these silent mutations strengthens one of the weak, central base-pairs: 3C converts U·G to C·G; 4A and 25C convert G·U to A·U or G·C. (iii) Mobility is regained when compensatory mutations are combined to reinstate the fourth or fifth base-pair of the stem of structure I. (iv) Fifteen out of 16 mutations in the single-stranded regions of structure I (the 5′ loop, the 3′ terminator loop, and the hinge between the two stems) do not affect mobility. The exception is 12A, which had a small effect (μ = −3), perhaps because it potentiates an alternative structure (see above). The mutations in the hinge region (31G, 32G, and 31G/32G) are of special interest because they are predicted to disrupt one or both G·C base-pairs in the stem of structure II. Hence, the fact that these mutations are silent argues strongly against structure II. Another argument against structure II is the fact that the 32G mutation does not compensate for the 4C mutation. (v) Six mutants had two minor bands running ahead of the major bands. These minor bands might result because the mutation potentiates a novel alternative structure. For example, the 25G and 25A mutations might allow an extended structure II′ in which the mutant base is paired with 12U.

There is an excellent correlation between the effect of each mutation on mobility and its effect on *sar* RNA activity in vivo (Table 1). Mutations that disrupt the stem of structure I cause a severe defect in repression. Mutations in the stem or hinge that allow formation of structure I have little effect on repression. Compensatory pairs of mutations that fully or partially restore mobility also fully or partially restore activity in vivo. These results argue strongly that structure I forms in vivo, and that formation of the 5′ stem (but not its exact sequence) is critical for efficient repression by *sar* RNA. This pattern applies not only to the subset of mutations listed in Table 1, but to the other *sar* mutants as well (19; Jacques and Susskind, ms in prep.). The role of the 5′ stem-loop in stability of *sar* RNA to degradation in vivo and in efficient pairing with *ant* mRNA will be discussed elsewhere.

Mutations that disrupt structure I have variable effects on mobility, with μ ranging from −4 to −11. The decrease in mobility is generally greater for mutations disrupting both structures (μ = −7 to −11; positions 4 and 5) than for mutations disrupting structure I but not II (μ = −4 to −7; positions 1, 24, 25, and 28). Hence, when structure I is blocked, at least some of the latter mutants might adopt structure II instead, assuming that II migrates more slowly than I, but faster than whatever structure is adopted when neither I nor II can form.

Surprisingly, mobility of *sar* RNA is not affected when the third base-pair of structure I is changed from U·G to C·G, or when the fourth base-pair is changed from G·U to A·U, G·C, or C·G (Fig. 5). Thus, at these positions, strong and weak base-pairs appear to be equivalent. In contrast, at the fifth position, the strength of the base-pair affects mobility: G·C = C·G > A·U > G·U (Fig. 6). Since context effects are well established, it is plausible that different positions of the stem differ in significance. In particular, it is reasonable that loss of the strong G·C base-pair at the fifth position of the stem (which already contains two G·U and two A·U base-pairs) could be more influential than acquisition of a strong base-pair at the third or fourth position.

Gel mobility: a technique to probe RNA secondary structures

It has long been known that strong stem-loop structures in single-stranded RNA or DNA can cause band compressions in sequencing gels, despite the presence of high concentrations of urea and high running temperatures (9–12). In these cases, formation of a stem-loop structure makes the RNA or DNA migrate faster than its true size would predict.

Effects of secondary structure on mobility in non-denaturing gels have not been studied in great detail. Several groups have examined the mobility of synthetic RNA or DNA duplexes interrupted by bulges or interior loops (20–23). Bulges (unpaired bases in one strand only) retard mobility in non-denaturing gels, an effect that is attributed to kinking of the molecule induced by the bulge. In contrast, interior loops (mismatched bases in both strands) have little effect on mobility of otherwise duplex molecules. Other recent studies have shown that single nucleotide changes often result in detectable mobility shifts of single-stranded DNA fragments on non-denaturing gels (24). This phenomenon provides a remarkably simple method to detect and localize mutations. Though the basis of these mobility shifts has not been demonstrated, these 'conformational polymorphisms' are presumed to be due to effects of the mutations on secondary structure of the single-stranded DNA.

We have shown here that electrophoretic mobility on non-denaturing gels can be used to analyze the effects of mutations on the secondary structure of a small, natural RNA. It is hoped that this rapid and convenient method will prove useful for probing the structures of other natural RNAs. We note that the correct structure of *sar* RNA was deduced after only a few mutants had been analyzed. At present, it is impossible to predict how generally applicable this approach will be. Several caveats are worth noting. Although the 5′ stem-loop of *sar* RNA enhances mobility (as is the case for band compressions on sequencing gels), formation of secondary or tertiary structures might sometimes retard mobility. For *sar* RNA, mobility shifts are affected by the temperature of electrophoresis; we expect that the optimal temperature for analyzing mobility of other RNAs will vary, depending on the strength of the secondary structures involved. Other potentially critical variables include pH, ionic strength, and the presence or absence of Mg^{2+}. As discussed above, the genetic phenotypes of the *sar* mutants in vivo (Table 1) provide strong evidence that the structure deduced from mobility shifts is correct and physiologically relevant. Such tests of the validity of secondary structures will be necessary to verify the utility of the method.

ACKNOWLEDGMENTS

We thank J.Ding and C.A.Gross for generously providing RNA polymerase, and W.R.McClure for critical reading of the manuscript. This work was supported by National Institutes of Health grant GM36811 to M.M.S.

REFERENCES

1. Liao, S.-M., Wu, T., Chiang, C.H., Susskind, M.M. and McClure, W.R. 1987. Genes Develop. **1**:197–203.
2. Wu, T., Liao, S.-M., McClure, W.R. and Susskind, M.M. 1987. Genes Develop. **1**:204–212.
3. Simons, R.W. and Kleckner, N. 1988. Annu. Rev. Genet. **22**:567–600.
4. Case, C.C., Roels, S.M., Jensen, P.D., Lee, J., Kleckner, N. and Simons, R.W. 1989. *EMBO J.* **8**:4297–4305.
5. Tinoco, I. Jr., Borer, P.N., Dengler, B., Levine, M.D., Uhlenbeck, O.C., Crothers, D.M. and Gralla, J. 1973. *Nature New Biol.* **246**:40–41.
6. Turner, D.H., Sugimoto, N. and Freier, S.M. 1988. *Ann. Rev. Biophys. Biophys. Chem.* **17**:167–192.
7. Liao, S.-M. and McClure, W.R. 1989. In Gold, L. (ed.) Molecular Biology of RNA, Alan R. Liss, New York, N.Y., pp. 289–297.
8. Susskind, M.M. and Franko, M. 1988. In Melton, D.A. (ed.) Antisense RNA and DNA, Cold Spring Harbor Laboratory, Cold Spring Harbor, N.Y., pp. 23–28.
9. Kramer, F.R. and Mills, D.R. 1978. Proc. Natl. Acad. Sci. USA. **75**:5334–5338.
10. Mills, D.R. and Kramer, F.R. 1979. Proc. Natl. Acad. Sci. USA. **76**:2232–2235.
11. Maxam, A.M. and Gilbert, W. 1980. Meth. in Enzymol. **65**:499–560.
12. Gough, J.A. and Murray, N.E. 1983. *J. Mol. Biol.* **166**:1–19.
13. Jacques, J.-P. and Susskind, M.M. 1990. Genes Develop. **4**:1801–1810.
14. Higuchi, R., Krummel, B. and Saiki, R.K. 1988. *Nucleic Acids Res.* **16**:7351–7367.
15. Graña, D., Youderian, P. and Susskind, M.M. 1985. Genetics **110**:1–16.
16. Graña D., Gardella, T. and Susskind, M.M. 1988. *Genetics* **120**:319–327.
17. Knight, K.L., Bowie, J.U., Vershon, A.K., Kelley, R.D. and Sauer, R.T. 1989. J. Biol. Chem. **264**:3639–3642.
18. Smith, H.O. and Levine, M. 1964. *Proc. Natl. Acad. Sci. USA.* **52**:356–363.
19. Jacques, J.-P. 1990. Ph.D. thesis, Univ. of Southern California, Los Angeles, CA.
20. Bhattacharyya, A. and Lilley, D.M.J. 1989. *Nucleic Acids Res.* **17**:6821–6840.
21. Bhattacharyya, A., Murchie, A.I.H. and Lilley, D.M.J. 1990. *Nature* **343**:484–487.
22. Hsieh, C.-H. and Griffith, J.D. 1989. Proc. Natl. Acad. Sci. USA **86**:4833–4837.
23. Rice, J.A. and Crothers, D.M. 1989. *Biochemistry* **28**:4512–4516.
24. Orita M., Iwahana, H., Kanazawa, H., Hayashi, K. and Sekiya, T. 1989. *Proc. Natl. Acad. Sci. USA* **86**:2766–2770.